

Graph Cut Energy Minimization in a Probabilistic Learning Framework for 3D Prostate Segmentation in MRI

S. Ghose^{1,2}, J. Mitra^{1,2}, A. Oliver², R. Martí², X. Lladó², J. Freixenet²,
J. C. Vilanova³, D. Sidibé¹, and F. Meriaudeau¹

¹ Univ. de Bourgogne, France, ² Univ. de Girona, Spain, ³ Girona Magnetic Resonance Center, Spain.
(soumya.ghose/jhimli.mitra/dro-desire.sidibe/fmeriau)@u-bourgogne.fr; (aoliver/marly/llado)@eia.udg.edu

*

Abstract

Variations in inter-patient prostate shape, and size and imaging artifacts in magnetic resonance images (MRI) hinders automatic accurate prostate segmentation. In this paper we propose a graph cut based energy minimization of the posterior probabilities obtained in a supervised learning schema for automatic 3D segmentation of the prostate in MRI. A probabilistic classification of the prostate voxels is achieved with a probabilistic atlas and a random forest based learning framework. The posterior probabilities are combined to obtain the likelihood of a voxel being prostate. Finally, 3D graph cut based energy minimization in the stochastic space provides segmentation of the prostate. The proposed method achieves a mean Dice similarity coefficient (DSC) value of 0.91 ± 0.04 and 95% mean Hausdorff distance (HD) of 4.69 ± 2.62 voxels when validated with 15 prostate volumes of a public dataset in a leave-one-patient-out validation framework. The model achieves statistically significant t-test p-value < 0.0001 in mean DSC and mean HD values compared to some of the works in literature.

1. Introduction

Prostate segmentation in MRI facilitates volume estimation, multi-modal image registration, surgical planning and image guided prostate biopsies. Manual segmentation of the prostate in MRI is time consuming and suffers from inter and intra-observer variabilities. However, inter-patient prostate shape, size, deformation and intensity variations along with imaging artifacts challenge 3D automatic segmentation of the prostate. Atlas

based prostate segmentation have achieved good segmentation accuracies when validated with large number of MRI datasets [6]. Motivated by these approaches we propose a probabilistic classification of the prostate voxels achieved by the fusion of the posterior probabilities determined with a probabilistic atlas and a supervised learning framework of random forest. Finally, graph cut based energy minimization [1] of the posterior probabilities produces the 3D segmentation of the prostate. The proposed method is robust to inter-patient shape, size and intensity variabilities. The key contributions of this work are: (1) Fusion of the posteriors from random forest and probabilistic atlas to achieve probabilistic classification of the prostate. (2) Use of graph cut in the stochastic domain to achieve segmentation of the prostate.

2. Proposed Segmentation Framework

The proposed method is developed on three major components: 2.1) Probabilistic atlas based segmentation, 2.2) Random forest based probabilistic classification of the voxels being prostate, and 2.3) Graph cut based energy minimization of the combined probabilities. The schema of our proposed method is illustrated in Fig. 1.

2.1 Probabilistic Atlas

The demons energy [9] is computed from the difference of voxel intensities between the moving and reference volumes. The minimization of the energy gradient provides the corresponding update (U) of a given transformation field (S). Edge forces of both the moving and reference volumes improve the registration convergence and stability. If M and F represent the moving and reference volumes respectively, then the voxel velocity u at voxel p with m and f as the respective voxel intensities is given by Eq. (1) and the demons energy $E(u)$ is

*Thanks to VALTEC 08-1-0039 of Generalitat de Catalunya, Spanish Science and Innovation grant nb. TIN2011-23704, Spain and Conseil Régional de Bourgogne, France for funding the research.

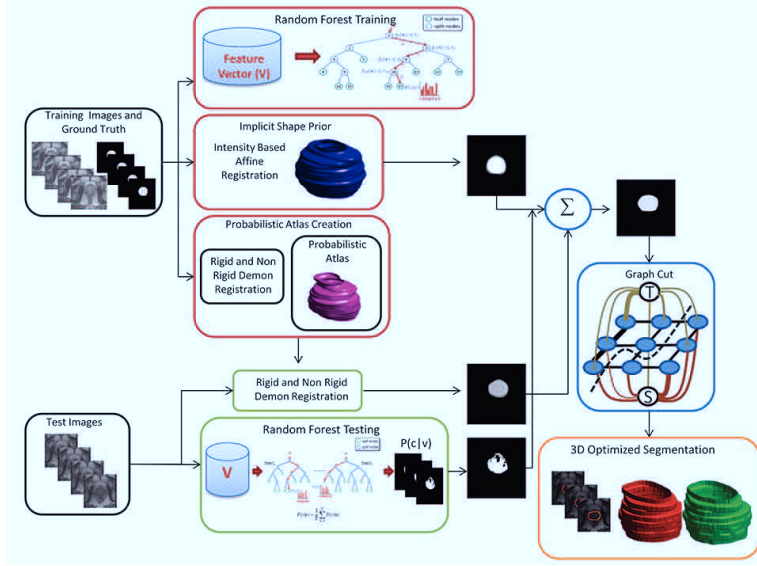


Figure 1. Schematic representation of our approach. Posteriors from shape restricted random forest classification and probabilistic atlas based segmentation are combined (Σ). Graph cut based energy minimization of the combined probabilities provides the segmentation. The green contour/volume is created from the ground truth and red contour/volume is created from obtained segmentation.

given by Eq. (2).

$$u = \frac{(m-f)\nabla f}{|\nabla f|^2 + \alpha(m-f)^2} + \frac{(m-f)\nabla m}{|\nabla m|^2 + \alpha(m-f)^2} \quad (1)$$

$$E(u) = \|F - M \circ (S + U)\|^2 + \frac{\sigma_i^2}{\sigma_x^2} \|U\|^2. \quad (2)$$

where ∇f and ∇m are the respective intensity gradients and α is a normalization factor that adjusts the force strength, σ_i^2 and σ_x^2 are the constants for intensity and transformation uncertainties respectively. The process of atlas construction begins with alignment of N manually segmented training datasets to a common reference. One among N training datasets is manually selected by an expert to reduce bias and $N - 1$ datasets are registered to the reference dataset. The registration is done in two stages, intensity based affine registration of $N - 1$ datasets to the reference dataset is followed by the non-rigid demons registration. The mean volume is computed by averaging all patient volumes aligned to the reference volume. The probability map is obtained by averaging the deformed patient volume labels. Given a new patient dataset, the atlas is first registered to the dataset using affine and demons based registration. Once registered, the transformation of the atlas probability map determines the probabilistic segmentation of the new patient dataset given by P_{at} . Following [6, 7] we manually select the volume-of-interest encompassing the prostate, the bladder and the rectum to reduce the computational time.

2.2 Random Forest Based Classification

MRI intensities of the prostate and the background regions are difficult to differentiate. Also the inter-patient intensities inside the prostate region may vary significantly depending on the acquisition parameters and imaging artifacts. Such intensity variations may affect graph cut based energy minimization framework. Therefore, to reduce the intensity variations and significantly differentiate between the prostate and the background regions we propose to substitute intensities with posterior probabilities of a voxel being prostate. Our probabilistic classification problem is addressed in a supervised learning schema of random decision forest [4].

The training phase begins with the normalization of intensities of the training volumes of interest and with their rigid alignment to minimize the pose and intensity variations. The data for training consists of a collection of $3 \times 3 \times 3$ neighborhood of voxels, centered at $V = (X, F)$, with $X = (x, y, z)$ denoting the position of the voxel associated with a feature vector F . The feature vector F consists of the mean and standard deviation of the $3 \times 3 \times 3$ voxel neighborhood. Each tree t in a decision forest of T trees receives the full data set of V along with the label and selects a test to split V into two subsets to maximize information gain where, a test is a feature response threshold. The left and the right child nodes receive their respective subsets of V and the process is repeated at each child node to grow the tree. The growth is terminated if either the information gain is minimum or the tree has grown to a max-

imum specified depth. Each decision tree in the forest is unique as each tree node selects a random subset of features and threshold.

During testing, the manually selected volume of interest of the test dataset encompassing the prostate, the bladder and the rectum with normalized intensities is rigidly aligned to the pre-registered training data. Each voxel of the test dataset is propagated through all the trees by successive application of the relevant binary test to determine the probability of belonging to class c . When reaching a leaf node l_t in all tree with $t \in [1, \dots, T]$, posterior probabilities ($P_t(c|V)$) are gathered in order to compute the final posterior probability of the voxel defined by $P(c|V) = \frac{1}{T} \sum_{t=1}^T P_t(c|V)$. Geremia et al. [4] imposed spatial restriction on the classified voxels by incorporating spatial information of the voxels obtained from the atlas. Similarly, to impose probabilistic implicit shape and spatial prior to the decision forest classification, we obtain a probabilistic shape and spatial prior model P_{sp} of the prostate by averaging the intensity-based affine registration of the ground truth obtained from the training datasets. P_{sp} is aligned with the center of the volume obtained from decision forest classification and the shape and spatial priors are imposed on the random forest classification by obtaining the likelihood value of a voxel being prostate as $P_{lk} = P(c|V) \times P_{sp}$.

Probabilistic segmentation of the prostate obtained using a probabilistic atlas (P_{at}) is fused with the likelihood values P_{lk} to achieve the final probabilistic classification of the prostate by $P_{fn} = \log(P_{at}) + \log(P_{lk})$. Log likelihood minimizes the effect of error incorporated either from the demon registration or from the random forest classification.

2.3 Graph Cut Based Energy Minimization

Our segmentation problem may be formulated as Maximum A Posteriori estimation of a Markov random field and could be solved in a graph cut energy minimization framework [1]. The graph $G = \langle Vx, \epsilon \rangle$ is defined as set of voxels Vx and a set of edges ϵ connecting neighboring voxels where the objective is to compute the best cut that minimizes the sum of the costs of the edges. Close neighboring voxels have higher edge costs. Two specially designated terminal nodes Sr (source) and Ta (sink) that represent the prostate and the background have to be manually selected by the user. However, we use soft classification of the prostate to automatically determine Sr and Ta . Typically, the neighboring voxels are interconnected by edges in a regular grid like structure. The objective of graph cut based energy minimization is to completely separate the terminals Sr and Ta , thereby segmenting the prostate from the background. In our model, we build the graph with soft classification of the voxels and use graph cut over the soft classification to achieve the final 3D seg-

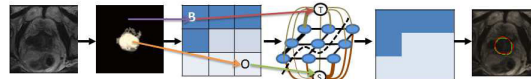


Figure 2. $Sr(S)$ and $Ta(T)$ terminals are identified automatically from posterior probabilities. Graph cut based energy minimization in 3D provides the segmentation.

mentation of the prostate. Our model could be formalized as; let a be a voxel and B be the set of all voxels and x_a be 0 or 1 depending on a belonging to the background or the prostate. Let E^a be the individual voxel matching cost for a ; $E^{a,c}$ vary inversely with the difference of intensities of voxels a and c . Then the cost function is given as,

$$E = \sum_{a \in B} E^a(x_a) + \sum_{(a,c) \in \epsilon} E^{a,c}(x_a, x_c) \quad (3)$$

where ϵ is the set edges of neighboring voxels. The first term represents the cost information related to data, while the second term represents a smoothness related cost. Energy E is minimized by max-flow/min-cut based graph cut [1]. Graph cut based energy minimization is illustrated in Fig. 2.

3. Experimental Results and Discussions

We have validated the accuracy and robustness of our approach with the 15 MRI public dataset of MICCAI prostate challenge [8] in a leave-one-patient-out validation strategy. During validation, probabilistic atlas and decision forest are build with 14 training datasets as discussed in sections 2.1 and 2.2. The number of trees were fixed to 100, tree depth to 30 and the lower bound of information gain to 10^{-7} in decision forest as these parameters produced promising results with test images. The features of random forest were limited to mean and standard deviation of voxels. During testing, the probabilistic atlas is registered to the test dataset and the probabilistic labels are transformed to achieve a probabilistic segmentation of the prostate. Next a probabilistic classification of the voxels is achieved with shape restricted decision forest and atlas-based segmentation probabilities as discussed in 2.2. We have used the popular prostate segmentation evaluation metrics like Dice similarity coefficient (DSC), and 95% Hausdorff distance (HD) to evaluate our method. To have an overall quantitative estimate of our performance we have compared our method with the results published in the MICCAI prostate challenge 2009 [7, 2], with the work of Gao et al. [3] and with the work of Ghose et al. [5] in Table 1. Please note that [2] used a probabilistic atlas for their segmentation achieving a DSC value of 0.73; however, our stochastic framework which combines the probabilities from decision forest and probabilistic atlas produces better results (DSC 0.91). In fact,

Table 1. Prostate segmentation quantitative results.

VOI=Volume of interest			
Method	DSC	HD	Manual Interaction
Merida [7]	0.79	7.11 mm	Selection of VOI
Dowling [2]	0.73±0.11	-	Selection of VOI
Gao [3]	0.82±0.05	10.22±4.03	Initialization
Ghose [5]	0.88±0.11	6.18±5.15	Initialization
Our Method	0.91±0.04	4.69±2.62	Selection of VOI

statistically significant improvement in DSC and HD of student P test t-value < 0.0001 has been achieved compared to [2, 3]. Moreover [3] used shape and local region based statistics of mean and standard deviation of the voxels to propagate their levelsets to achieve a deterministic segmentation of the prostate. We use similar features but employ a stochastic approach and use a MAP-MRF approach to compensate mis-classifications and achieve better results. Comparing our results to our previous work of [5] we observe that error in initialization of our shape and intensity prior model away from the center of gravity due to slice propagation adversely affected results. The combined framework of probabilistic atlas and random forest works as the two approaches produces better results in different zones of the prostate. The probabilistic atlas produces good results in the central region of the prostate while random forest produces better results in the base and the apex regions. Quantitatively, atlas based registration produces a DSC of value of 0.74 ± 0.18 , random forest produces a DSC value of 0.78 ± 0.25 , with average model refinement of random forest classification a DSC of 0.81 ± 0.15 is achieved and combining the two probabilities in log scale produced DSC of 0.87 ± 0.09 is obtained. Finally graph cut optimization further refines mis-classifications and produces a DSC of 0.91 ± 0.04 . Qualitative results are presented in Fig. 3.

4 Conclusions

A novel schema of graph cut based energy minimization in a stochastic domain obtained with atlas based segmentation and shape constrained decision forest with the goal of segmenting the prostate in MRI has been proposed. Our method is robust to significant shape, size and contrast variations in MRI compared to some existing work in the literature. The proposed method has shown promising results however the algorithm should be validated with more datasets and optimal feature selection may improve the probabilistic classification of the random forest. Furthermore the sensitivity analysis of manual interaction for model initialization needs to be studied and the effect of using other registration methods like B-spline based image

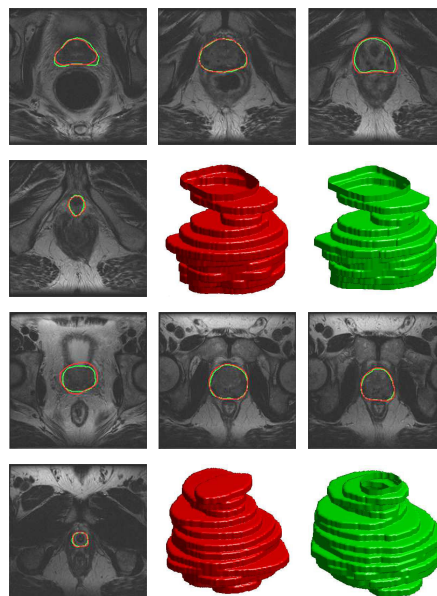


Figure 3. Subset of segmentation results of 2 datasets. The green contour/volume is created from the ground truth and red contour/volume is created from obtained segmentation.

registration needs to be analyzed.

References

- [1] Y. Boykov et al. Graph cuts and efficient n-d image segmentation. *Int. Jnl. of Comp. Vis.*, 70(2):109–131, 2006.
- [2] J. Dowling et al. Automatic atlas-based segmentation of the prostate. www.wiki.namic.org/Wiki/images/f/f1/Dowling_2009_MICCAIProstate_v2, Accessed on [20th Jan, 2012].
- [3] Y. Gao et al. A Coupled Global Registration and Segmentation Framework with Application to Magnetic Resonance Prostate Imagery. *IEEE Trans. on Med. Imag.*, 10:17–81, 2010.
- [4] E. Geremia et al. Spatial decision forests for ms lesion segmentation in multi-channel MR images. In *MICCAI*, volume 6361, pages 111–118, 2010.
- [5] S. Ghose et al. A hybrid framework of multiple active appearance models and global registration for 3D prostate segmentation in MRI. In *SPIE Medical Imaging*, volume 8314, pages 8314S1–8314S9, 2012.
- [6] S. Klein et al. Automatic Segmentation of the Prostate in 3D MR Images by Atlas Matching Using Localized Mutual Information. *Med. Phys.*, 35:1407–1417, 2008.
- [7] A. Gubern-Merida et al. Atlas Based Segmentation of the Prostate in MR Images. www.wiki.namic.org/Wiki/images/d/d3/Gubern-Merida_Paper, accessed on [20th Jan, 2012].
- [8] MICCAI. 2009 prostate segmentation challenge MICCAI. <http://wiki.na-mic.org/Wiki/index.php>, accessed on [1st April, 2011], 2009.
- [9] J.-P. Thirion. Image matching as a diffusion process: an analogy with maxwell’s demons. *Med. Img. Anal.*, 2(3):243–260, 1998.